

# New Tsallis agegraphic Dark Energy in Horava-Lifshitz cosmology

M. Abdollahi Zadeh\*

*Not affiliated with any institution, Kazerun, Iran.*

We investigate the new Tsallis agegraphic dark energy (NTADE) scenario in the framework of Horava-Lifshitz cosmology. Considering interacting and non-interacting scenarios of NTADE with dark matter in a spatially non-flat universe, we investigate the cosmological implications of this model in detail. We obtain the differential equation of the evolution of the density parameter, the equation of state parameter and the classical stability of model. Also, we study the behavior of the deceleration parameter and investigate the nature of the statefinder diagnostics and  $\omega_D - \omega_D'$  plane. We find that phantom crossing cannot occur for the state parameter in this scenario and from the plot of the deceleration parameter, we have observed a transition from decelerating to accelerating phase of the universe. Also, the sign of the square of the sound speed is negative which means unstable behavior at this scenario. The  $\omega_D$  and  $\omega_D'$  have negative values which represents the freezing region at here.

## I. INTRODUCTION

Twenty years ago, two groups discovered independently that the Universe has entered a phase of accelerated expansion with a redshift between .5-1 [1, 2]. Since ordinary matter, such as baryon, has a positive pressure, it cannot accelerate the expansion of the Universe, so it must provide an unusual, unknown substance, called dark energy, the invisible fuel for this accelerated expansion [3, 4]. The simplest model to solve this problem is to consider vacuum energy as this invisible fuel but, assuming, we face two problems of fine-tuning and cosmic coincidence.

Thus, dynamical dark energy models become popular, what those models that originate from various fields, what those models that probe the nature of DE, according to some basic quantum gravitational principles. One example of latter paradigm is the agegraphic DE (ADE) model which has originated from quantum gravity and possesses some of its significant features. In this model, the age of the Universe  $T = \int dt$  is used as the IR cutoff  $L$  [5]. But this scenario cannot justify the matter-dominated era, thus it was generalized to the agegraphic dark energy, namely the use of the conformal time  $\eta$  as the IR cutoff  $L$  [6, 7].

On the other hand, a theory of gravity renormalizable with higher spatial derivatives in four dimensions which is also similar to a scalar field theory of Lifshitz [8], in which the time dimension has weight 3 if a space dimension has weight 1, almost ten years ago was proposed by Horava [9], for this reason, this theory is called Horava-Lifshitz gravity. In the expression of characteristics of this theory can be said that, the causal structures of this theory are different from those present in General Relativity [10], because this theory is not Lorentz invariant and since it is non-relativistic, consequently, the speed of light  $c$  diverges in the Ultra-Violet (UV) limit. For

a recent review on Horava-Lifshitz (HL) gravity [11–13] and its application as the cosmological framework of the Universe see [14–25]. The logarithmic new agegraphic dark energy model has been studied in the framework of Horava-Lifshitz cosmology [26]. The generalized second law of thermodynamics and new agegraphic dark energy model have also been checked in Horava-Lifshitz cosmology [27, 28]. Solving the flatness problem with an anisotropic instanton in HL gravity has been studied in [29]. In [30] it is analyzed the electromagnetic-gravity interaction in HL framework. A noncommutative version of Friedmann Robertson-Walker (FRW) cosmological models in HL theory has been studied in [31] as well as the Hamiltonian dynamics of bouncing Bianchi IX cosmologies is examined [32]. The phase space analysis of Horava-Lifshitz cosmology for a wide range of self-interacting potentials has been studied in [33] as well as bouncing cosmology for entropy corrected models in Horava-Lifshitz gravity has also been checked in [34]. Similarly to the black hole, we use holographic principle in the cosmological applications, because of the fact that the entropy of the Universe can be counted by assuming that the universe is seen as a two-dimensional structure on the horizon of cosmology. Gibbs in his book with title “Elementary Principles in Statistical Mechanics” [35] pointed out that systems have a long range interaction, such as gravitation, do not necessarily obey the Boltzmann-Gibbs (BG) theory, and indeed these systems can violate the extensivity constraint of the Boltzmann-Gibbs entropy. On this basis, Tsallis in 1988 [36], introduced a non-additive entropy for the non-extensive systems which can be written in compact form as [37]

$$S_T = \gamma A^\delta, \quad (1)$$

where  $\gamma$  is an unknown constant and  $\delta$  denotes the non-extensive parameter. Recently, using relation (1) and holographic hypothesis, led to the suggestion of a dark energy density in the form

$$\rho_D = BL^{2\delta-4}, \quad (2)$$

where  $B$  is an unknown parameter, and it attracts more attempts to itself [38–60]. Here, we are interested in

---

\*mazkph@gmail.com

studying some cosmological consequences by considering the conformal time as the IR cut off in background Horava-Lifshitz cosmology.

The paper is organized as follows. In section II, we present Horava-Lifshitz cosmology and we analyze the new Tsallis agegraphic dark energy in Horava-Lifshitz cosmology, both in the simple and in the interacting forms. Beside extracting the differential equation that determines the evolution of the dark energy density parameter, as well as we investigate the model by using the statefinder diagnostic and  $\omega - \omega'$  analysis in section III. The conclusions are given in section IV.

## II. HORAVA-LIFSHITZ COSMOLOGY

We begin with a brief review of the cosmological model based on Horava-Lifshitz gravity [61]. What the projectability condition dictates is that the lapse function  $N$  should be space-independent, while the shift vector  $N^i$  and the 3-dimensional metric  $g_{ij}$  are dependent on both time and space. In terms of these dynamical variables, the full metric is parametrized as

$$ds^2 = -N^2 dt^2 + g_{ij}(dx^i + N^i dt)(dx^j + N^j dt), \quad (3)$$

### A. Detailed balance

The gravitational action of HL gravity based on a kinetic and a potential part can be expressed as  $S_g = \int dt d^3x \sqrt{g} N (\mathcal{L}_K + \mathcal{L}_V)$  and under the assumption of detailed balance [62], the full action of HL gravity can be written as follow

$$S_g = \int dt d^3x \sqrt{g} N \left\{ \frac{2}{\kappa^2} (K_{ij} K^{ij} - \lambda K^2) + \frac{\kappa^2}{2w^4} C_{ij} C^{ij} + L1 \right\} \quad (4)$$

$$L1 = -\frac{\kappa^2 \mu}{2w^2} \frac{\epsilon^{ijk}}{\sqrt{g}} R_{il} \nabla_j R_k^l + \frac{\kappa^2 \mu^2}{8} R_{ij} R^{ij}$$

$$L2 = +\frac{\kappa^2 \mu^2}{8(3\lambda - 1)} \left[ \frac{1 - 4\lambda}{4} R^2 + \Lambda R - 3\Lambda^2 \right],$$

where  $K_{ij}$  is the extrinsic curvature which takes the form

$$K_{ij} = \frac{1}{2N} (\dot{g}_{ij} - \nabla_i N_j - \nabla_j N_i) \quad (5)$$

and a dot denotes a derivative with respect to  $t$  and covariant derivatives defined with respect to the spatial metric  $g_{ij}$ . Also

$$C^{ij} = \frac{\epsilon^{ijk}}{\sqrt{g}} \nabla_k (R_i^j - \frac{1}{4} R \delta_i^j) \quad (6)$$

is the Cotton tensor,  $\lambda$ ,  $\epsilon^{ijk}$  and  $\Lambda$  are a dimensionless constant, the totally antisymmetric unit tensor and the

cosmological constant, respectively. Finally, the variables  $\kappa$ ,  $w$  and  $\mu$  are constant parameters with mass dimensions  $-1$ ,  $0$  and  $1$ , respectively. For focussing on cosmological contents, we should impose the so called projectability condition [61] under the detailed balance, then we consider a Friedmann-Robertson-Walker (FRW) metric,

$$N = 1, \quad g_{ij} = a^2(t) \gamma_{ij}, \quad N^i = 0, \quad (7)$$

with

$$\gamma_{ij} dx^i dx^j = \frac{dr^2}{1 - kr^2} + r^2 d\Omega_2^2, \quad (8)$$

where  $k = -1, 0, +1$  refer to spatially open, flat, and closed universe respectively. Taking the variation of action with respect to the metric components  $N$  and  $g_{ij}$ , we can obtain the equation of motion as

$$H^2 = \frac{\kappa^2}{6(3\lambda - 1)} \rho_m + \frac{\kappa^2}{6(3\lambda - 1)} \left[ \frac{3\kappa^2 \mu^2 k^2}{8(3\lambda - 1)a^4} + \frac{3\kappa^2 \mu^2 \Lambda^2}{8(3\lambda - 1)} \right] - \frac{\kappa^4 \mu^2 \Lambda k}{8(3\lambda - 1)^2 a^2} \quad (9)$$

$$\dot{H} + \frac{3}{2} H^2 = -\frac{\kappa^2}{4(3\lambda - 1)} p_m$$

$$-\frac{\kappa^2}{4(3\lambda - 1)} \left[ \frac{\kappa^2 \mu^2 k^2}{8(3\lambda - 1)a^4} - \frac{3\kappa^2 \mu^2 \Lambda^2}{8(3\lambda - 1)} \right] - \frac{\kappa^4 \mu^2 \Lambda k}{16(3\lambda - 1)^2 a^2} \quad (10)$$

where we have defined the Hubble parameter as  $H \equiv \frac{\dot{a}}{a}$  and  $a$  is scale factor. Also  $\rho_m$  and  $p_m$  are corresponding energy density and pressure of the matter. At this stage, by noticing the form of the preceding Friedmann equations, the energy density  $\rho_D$  and pressure  $p_D$  for dark energy can define as

$$\rho_D \equiv \frac{3\kappa^2 \mu^2 k^2}{8(3\lambda - 1)a^4} + \frac{3\kappa^2 \mu^2 \Lambda^2}{8(3\lambda - 1)} \quad (11)$$

$$p_D \equiv \frac{\kappa^2 \mu^2 k^2}{8(3\lambda - 1)a^4} - \frac{3\kappa^2 \mu^2 \Lambda^2}{8(3\lambda - 1)}. \quad (12)$$

It is interesting to note that the first term on the right-hand side proportional to  $a^{-4}$  is the usual ‘‘dark radiation term’’, present in Hořava-Lifshitz cosmology [61], while the second term is just the explicit cosmological constant. As a last step, these expressions reduce to the standard Friedmann equations ( $c = 1$ ), provided we consider [61]

$$G_{\text{cosmo}} = \frac{\kappa^2}{16\pi(3\lambda - 1)} \quad (13)$$

$$\frac{\kappa^4 \mu^2 \Lambda}{8(3\lambda - 1)^2} = 1, \quad (14)$$

where  $G_{\text{cosmo}}$  presents the Newton's cosmological constant. It is worth mentioning that in gravitational theories with the violation of Lorentz invariance,  $G_g$  in the gravitational action differs from  $G_{\text{cosmo}}$  in the Friedmann equations, unless Lorentz invariance is restored [63]. For completeness we define  $G_g$  as

$$G_g = \frac{\kappa^2}{32\pi}. \quad (15)$$

Clearly, in the IR limit ( $\lambda = 1$ ), where Lorentz invariance is restored,  $G_{\text{cosmo}}$  and  $G_g$  are the same.

Now, by using the above identifications, we can rewrite the modified Friedmann equations (9) and (10) in the standard form as

$$H^2 + \frac{k}{a^2} = \frac{8\pi G_{\text{cosmo}}}{3}(\rho_m + \rho_D) \quad (16)$$

$$\dot{H} + \frac{3}{2}H^2 + \frac{k}{2a^2} = -4\pi G_{\text{cosmo}}(p_m + p_D). \quad (17)$$

### III. NEW TSALLIS AGEGRAPHIC DARK ENERGY MODEL (NTADE)

Here we would like to study the NTADE [64] in HL theory, to do this, we consider a spatially non-flat Universe in which there are a new Tsallis agegraphic dark energy  $\rho_D$  and pressureless dark matter  $\rho_m$ . If we introduce the density parameters as

$$\Omega_m = \frac{8\pi G_{\text{cosmo}}}{3H^2}\rho_m, \quad \Omega_D = \frac{8\pi G_{\text{cosmo}}}{3H^2}\rho_D, \quad \Omega_k = \frac{k}{a^2H^2}, \quad (18)$$

then, the first Friedmann equation (16) can be rewritten as

$$1 + \Omega_k = \Omega_m + \Omega_D. \quad (19)$$

As mentioned earlier, because the original ADE model has some difficulties in particular, in to justify the matter-dominated era [65], it motivated Wei and Cai [6] to propose the new ADE model, while the time scale is chosen to be the conformal time instead of the age of the Universe. Considering the conformal time as IR cutoff which is defined as  $dt = ad\eta$  leading to  $\dot{\eta} = 1/a$  and thus

$$\eta = \int_0^a \frac{da}{Ha^2}. \quad (20)$$

Thus, the corresponding dark energy by considering Eq.(2) reads

$$\rho_D = B\eta^{2\delta-4}. \quad (21)$$

Taking time derivative of above equation and using  $\dot{\eta} = 1/a$ , we can obtain

$$\dot{\rho}_D = \frac{\rho_D(2\delta-4)}{a\eta}, \quad (22)$$

Also, if we take the time derivative of the second relation in (18) after using (22) and relation  $\dot{\Omega}_D = \Omega'_D H$ , we can obtain the equation of motion for  $\Omega_D$  as

$$\Omega'_D = 2\Omega_D \left( \frac{\delta-2}{a\eta H} - \frac{\dot{H}}{H^2} \right) \quad (23)$$

where prime denotes the derivative with respect to  $x = \ln a$ . As previous, by taking derivative of the third relation in (18) we get

$$\Omega'_k = -2\Omega_k \left( 1 + \frac{\dot{H}}{H^2} \right). \quad (24)$$

#### A. statefinder diagnostic and $\omega - \omega'$ analysis

However two cosmological parameters  $H$  and  $q$  are useful to describe the evolution of the Universe, but these two parameters cannot differentiate various dark energy models. For this reason, Sahni et al.,[66] introduced a new geometrical diagnostic pair parameter  $\{r, s\}$ , known as the statefinder pair, defined as

$$r = \frac{\ddot{a}}{aH^3}, \quad s = \frac{r-1}{3(q-1/2)}, \quad (25)$$

which clearly show the statefinder pair depend only on the scale factor and its time derivatives up to third order. Note that the parameter  $r$  is also called cosmic jerk and can be expressed in terms of the Hubble and the deceleration parameters as

$$r = 2q^2 + q - \frac{\dot{q}}{H}. \quad (26)$$

Before we apply the statefinder diagnostic to the NTADE model in HL gravity, it is better to note that i) in the  $\{r, s\}$  plane,  $s > 0$  ( $s < 0$ ) corresponds to a quintessence-like (phantom-like) model of DE respectively. ii) In a flat  $\Lambda$ CDM model and matter dominated universe (SCDM) one finds  $\{r, s\} = \{1, 0\}$  and  $\{r, s\} = \{1, 1\}$ , respectively. As a complement to statefinder diagnosis, the  $\omega_D - \omega'_D$  analysis is also useful method for distinguish different cosmological models [67]. In this approach i) the  $\Lambda$ CDM model corresponds to a fixed point  $\{\omega_D = -1, \omega'_D = 0\}$  in the  $\omega_D - \omega'_D$  plane, where  $\omega'_D$  represents the derivative of  $\omega_D$  with respect to  $x = \ln a$ . ii)  $\omega'_D > 0$  and  $\omega_D < 0$  present the thawing region. (iii)  $\omega'_D < 0$  and  $\omega_D < 0$  present the freezing region [67].

#### B. Non-interacting case ( $Q = 0$ )

As usual, in the new Tsallis agegraphic dark energy scenario, the energy densities for matter and dark energy obey the standard evolution equation:

$$\dot{\rho}_m + 3H(\rho_m + p_m) = 0, \quad (27)$$

$$\dot{\rho}_D + 3H(\rho_D + p_D) = 0, \quad (28)$$

where  $p_m$  is pressure of matter (here we take  $p_m = 0$ ) and  $p_D = \omega_D \rho_D$ , also,  $\omega_D$  is the equation of state (EoS) parameter of the NTADE model what can be achieved by inserting Eq.(22) in relation (28) as

$$\omega_D = -1 - \frac{2\delta - 4}{3a\eta H}, \quad (29)$$

where  $\eta = \left(\frac{3H^2\Omega_D}{8\pi G_{\text{cosmo}}B}\right)^{\frac{1}{2\delta-4}}$ . Also, the time derivative of Eq.(29) with respect to  $x = \ln a$ , we get

$$\omega'_D = \frac{(\delta - 2)(2 + 2(\delta - 2)\Omega_D + a\eta H(-1 + 3\Omega_D - \Omega_k))}{3a^2\eta^2 H^2}. \quad (30)$$

Taking the derivative of both side of the Friedmann equation (16) with respect to the cosmic time  $t$ , and using Eqs.(27) and (22) we find

$$\frac{\dot{H}}{H^2} = \Omega_k + \Omega_D \left(-\frac{3}{2}u + \frac{\delta - 2}{a\eta H}\right), \quad (31)$$

where  $u = \frac{\rho_m}{\rho_D} = -1 + \frac{1+\Omega_k}{\Omega_D}$  is the ratio of the energy densities. Finally, by substituting the above equation in relation

$$q \equiv -1 - \frac{\dot{H}}{H^2}, \quad (32)$$

we obtain the expression for the deceleration parameter as

$$q = -1 - \Omega_k + \Omega_D \left(\frac{3}{2}u + \frac{2 - \delta}{a\eta H}\right). \quad (33)$$

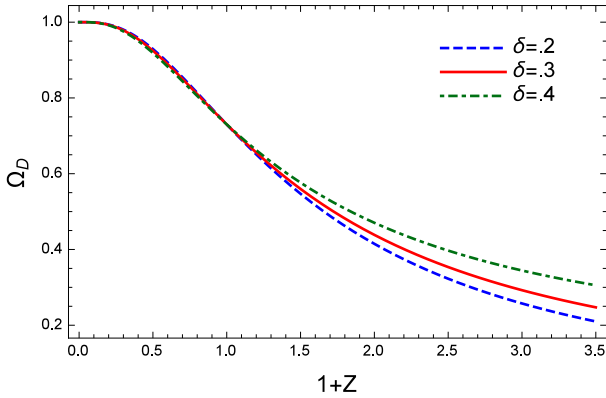


FIG. 1: The evolution of  $\Omega_D$  versus redshift parameter  $z$  for non-interacting NTADE in HL cosmology. Here, we have taken  $\Omega_D(z = 0) = 0.73$ ,  $H(z = 0) = 67$ ,  $\Omega_k(z = 0) = 0.01$ ,  $\lambda = 1.6$  and  $B = 2.4$  [68]

We now consider an important quantity to check the effects of perturbations on the classical stability of our model, namely the square of the sound speed  $v_s^2$ , defined as

$$v_s^2 = \frac{dP_D}{d\rho_D} = \frac{\dot{P}_D}{\dot{\rho}_D} = \frac{\rho_D}{\dot{\rho}_D} \dot{\omega}_D + \omega_D, \quad (34)$$

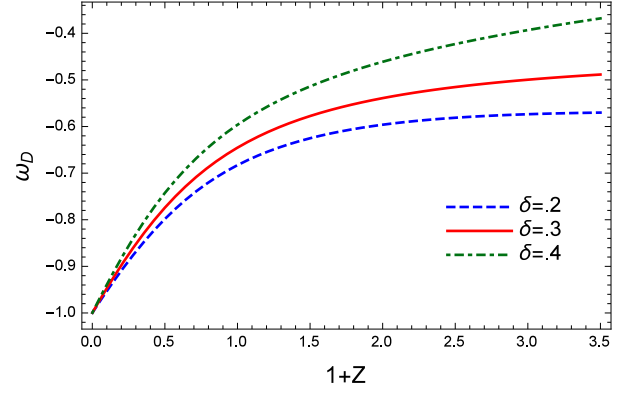


FIG. 2: The evolution of  $\omega_D$  versus redshift parameter  $z$  for non-interacting NTADE in HL cosmology. Here, we have taken  $\Omega_D(z = 0) = 0.73$ ,  $H(z = 0) = 67$ ,  $\Omega_k(z = 0) = 0.01$ ,  $\lambda = 1.6$  and  $B = 2.4$

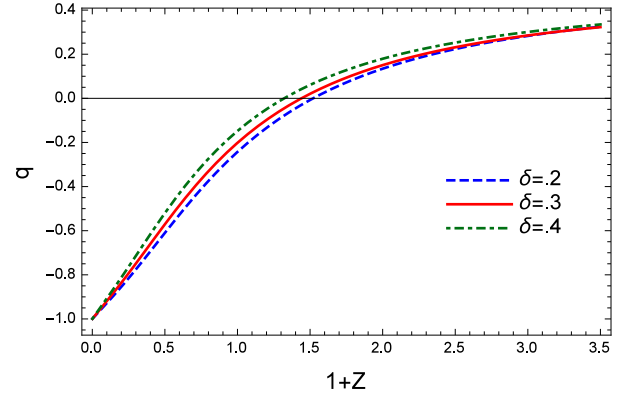


FIG. 3: The evolution of the deceleration parameter  $q$  versus redshift parameter  $z$  for non-interacting NTADE in HL cosmology. Here, we have taken  $\Omega_D(z = 0) = 0.73$ ,  $H(z = 0) = 67$ ,  $\Omega_k(z = 0) = 0.01$ ,  $\lambda = 1.6$  and  $B = 2.4$

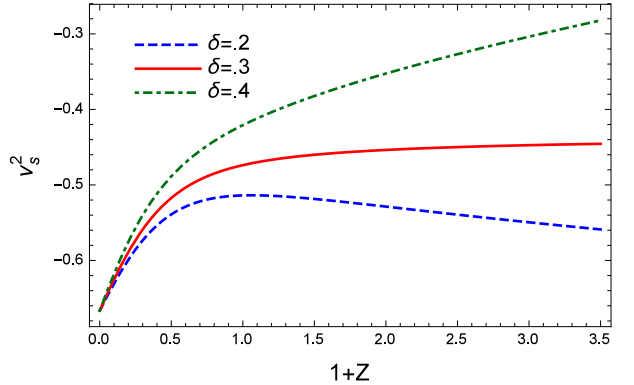


FIG. 4: The evolution of the squared of sound speed  $v_s^2$  versus redshift parameter  $z$  for non-interacting NTADE in HL cosmology. Here, we have taken  $\Omega_D(z = 0) = 0.73$ ,  $H(z = 0) = 67$ ,  $\Omega_k(z = 0) = 0.01$ ,  $\lambda = 1.6$  and  $B = 2.4$

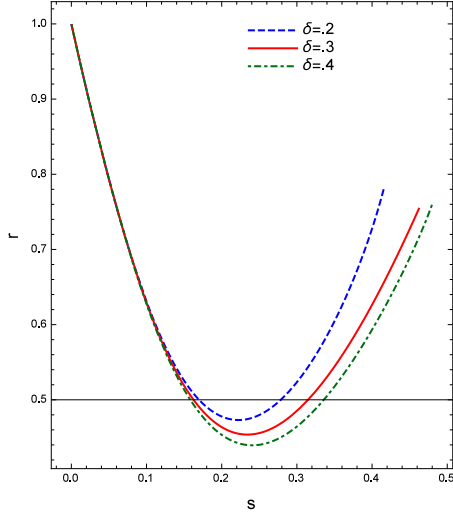


FIG. 5: The evolution of the statefinder parameter  $r$  versus  $s$  for non-interacting NTADE in HL cosmology. Here, we have taken  $\Omega_D(z=0) = 0.73$ ,  $H(z=0) = 67$ ,  $\Omega_k(z=0) = 0.01$ ,  $\lambda = 1.6$  and  $B = 2.4$

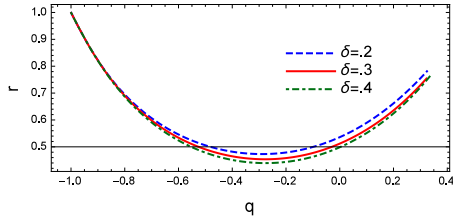


FIG. 6: The evolution of the statefinder parameter  $r$  versus the deceleration parameter  $q$  for non-interacting NTADE in HL cosmology. Here, we have taken  $\Omega_D(z=0) = 0.73$ ,  $H(z=0) = 67$ ,  $\Omega_k(z=0) = 0.01$ ,  $\lambda = 1.6$  and  $B = 2.4$

which finally leads to

$$v_s^2 = \frac{5 - 2\delta + (\delta - 2)\Omega_D}{3\eta a H} + \frac{-7 + 3\Omega_D - \Omega_k}{6}, \quad (35)$$

for the non-interacting case. The statefinder parameters for NTADE in HL are obtained in accordance with the equation (25) as

$$r = 1 + \Omega_k + \frac{(2 - \delta)\Omega_D(5 - 2\delta + (\delta - 2)\Omega_D)}{\eta^2 a^2 H^2} + \frac{(2 - \delta)\Omega_D(-7 + 3\Omega_D - \Omega_k)}{2\eta a H}, \quad (36)$$

$$s = \frac{(\delta - 2)\Omega_D(a\eta H(-7 + 3\Omega_D) + 2(5 - 2\delta + (\delta - 2)\Omega_D))}{3a\eta H((-4 + 2\delta + 3a\eta H)\Omega_D - a\eta H\Omega_k)} - \frac{(2a\eta H + (\delta - 2)\Omega_D)\Omega_k}{3((-4 + 2\delta + 3a\eta H)\Omega_D - a\eta H\Omega_k)}. \quad (37)$$

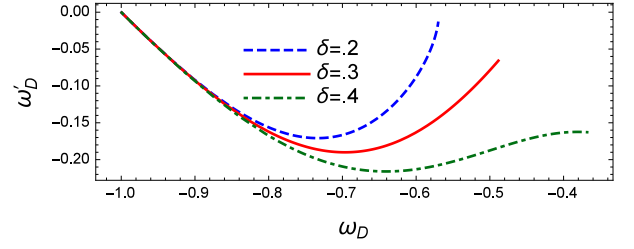


FIG. 7: The  $\omega_D - \omega'_D$  diagram for non-interacting NTADE in HL cosmology. Here, we have taken  $\Omega_D(z=0) = 0.73$ ,  $H(z=0) = 67$ ,  $\Omega_k(z=0) = 0.01$ ,  $\lambda = 1.6$  and  $B = 2.4$

The evolution of the system parameters for non-interacting case are plotted in Figs. 1-7. In Figs. 1-3, we plot the evolution of  $\Omega_D$ ,  $\omega_D$  and  $q$  versus redshift parameter  $z$  for non-interacting case. it is obvious that  $\Omega_D$  tends to 0 in the early universe,  $\omega_D$  cannot cross phantom line and the universe enter the acceleration phase earlier for smaller  $\delta$ . In Fig. 4 we show the evolution of  $v_s^2$ , which is unstable here. In Figs. 5-7, we also plot the trajectories of statefinder pair and  $\omega - \omega'$  plane. From trajectory of  $(r - s)$ , we see a quintessence-ilke behaviour as well as  $\omega - \omega'$  plane presents the freezing region.

### C. Interacting case ( $Q \neq 0$ )

Here, we postulate that the two sectors the NTADE and dark matter (DM) interact through the interaction term  $Q$ , since such a scenario could alleviate the known coincidence problem [69]. It should be noted that the recent observational evidence by the galaxy clusters supports the interaction between DE and DM [70]. This causes the energy conservation law for each dark component to be hold separately i.e.

$$\dot{\rho}_m + 3H\rho_m = Q, \quad (38)$$

$$\dot{\rho}_D + 3H(1 + \omega_D)\rho_D = -Q, \quad (39)$$

where  $Q$  has a form as follows  $Q = 3b^2 H\rho_m$  with  $b^2$  being a coupling constant. It deserves mention three cases a bout interaction term  $Q$  i) for  $Q > 0$ , there is an energy transfer from NTADE to DM. ii) the form of  $Q$  is chosen purely phenomenologically, in order to obtain desirable cosmological results including phantom crossing and accelerated expansion. iii) easily, one can find numerous form of  $Q(H\rho)$  in Ref[71–75].

By repeating the above procedure in the case where the matter and dark sectors are allowed to interact, we find expressions for cosmological application, similiary to the previous subsection,

$$\frac{\dot{H}}{H^2} = \Omega_k + \Omega_D \left( \frac{3}{2}u(b^2 - 1) + \frac{\delta - 2}{a\eta H} \right), \quad (40)$$

$$\omega_D = -1 - b^2 u - \frac{2\delta - 4}{3a\eta H}, \quad (41)$$

$$q = -1 - \Omega_k - \Omega_D \left( \frac{3}{2} u (b^2 - 1) + \frac{\delta - 2}{a\eta H} \right), \quad (42)$$

$$v_s^2 = \frac{5 - 2\delta + (\delta - 2)\Omega_D}{3\eta a H} + \frac{-3b^2(\Omega_D - 1 - \Omega_k) - 7 + 3\Omega_D - \Omega_k}{6} + \frac{3b^2(b^2 - 1)a\eta H(\Omega_D - 1 - \Omega_k)}{2(\delta - 2)\Omega_D}, \quad (43)$$

$$r = \frac{(2 - \delta)\Omega_D(5 - 2\delta + (\delta - 2)\Omega_D)}{\eta^2 a^2 H^2} + \frac{(2 - \delta)\Omega_D(-7 + 3\Omega_D - \Omega_k + 3b^2(1 - \Omega_D + \Omega_k))}{2\eta a H} + \frac{2(1 + \Omega_k) + 9b^2(b^2 - 1)(1 - \Omega_D + \Omega_k)}{2}, \quad (44)$$

$$s = \frac{M1 + M2}{M3}. \quad (45)$$

$$M1 = -2(\delta - 2)\Omega_D(5 - 2\delta + (\delta - 2)\Omega_D)$$

$$+ a\eta H \Omega_D (\delta - 2) (7 - 3b^2 + 3(b^2 - 1)\Omega_D + \Omega_k - 3b^2\Omega_k)$$

$$M2 = a^2 \eta^2 H^2 (-9b^2(b^2 - 1)(\Omega_D - 1) + (2 + 9b^2(b^2 - 1))\Omega_k)$$

$$M3 = 3a\eta H [-2(\delta - 2)\Omega_D + a\eta H (-3b^2 + 3\Omega_D(b^2 - 1) + m3)]^\sigma$$

$$m3 = +\Omega_k - 3b^2\Omega_k$$

In Figs. 8-14, we present system parameters for various values of  $b^2$  for interacting case.

In Fig. 9, we see that the equation of state  $\omega_D$  cannot cross phantom line as well as by considering different values of  $b^2$ , Fig. 11, shows unstability of this model. The evolutionary trajectories for  $(r - s)$  and  $(r - q)$  planes for TNADE model in HL cosmology have plotted in Figs. 12 and 13 respectively. Fig. 12, shows that, the evolutionary trajectories  $r$  and  $s$  end at  $\Lambda$ CDM ( $r = 1, s = 0$ ) in

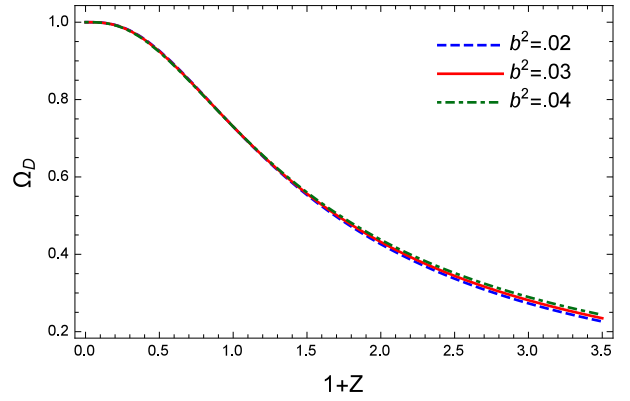


FIG. 8: The evolution of  $\Omega_D$  versus redshift parameter  $z$  for interacting NTADE in HL cosmology. Here, we have taken  $\Omega_D(z = 0) = 0.73$ ,  $H(z = 0) = 67$ ,  $\Omega_k(z = 0) = 0.01$ ,  $B = 2.4$ ,  $\lambda = 1.6$  and  $\delta = .2$

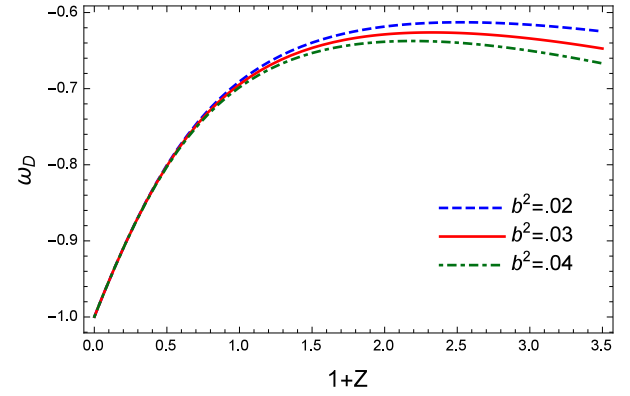


FIG. 9: The evolution of  $\omega_D$  versus redshift parameter  $z$  for interacting NTADE in HL cosmology. Here, we have taken  $\Omega_D(z = 0) = 0.73$ ,  $H(z = 0) = 67$ ,  $\Omega_k(z = 0) = 0.01$ ,  $B = 2.4$ ,  $\lambda = 1.6$  and  $\delta = .2$

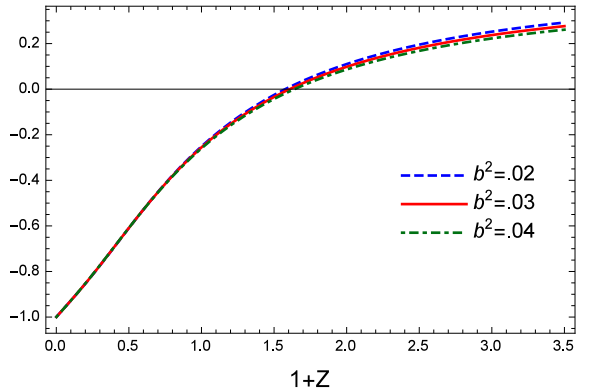


FIG. 10: The evolution of the deceleration parameter  $q$  versus redshift parameter  $z$  for interacting NTADE in HL cosmology. Here, we have taken  $\Omega_D(z = 0) = 0.73$ ,  $H(z = 0) = 67$ ,  $\Omega_k(z = 0) = 0.01$ ,  $B = 2.4$ ,  $\lambda = 1.6$  and  $\delta = .2$

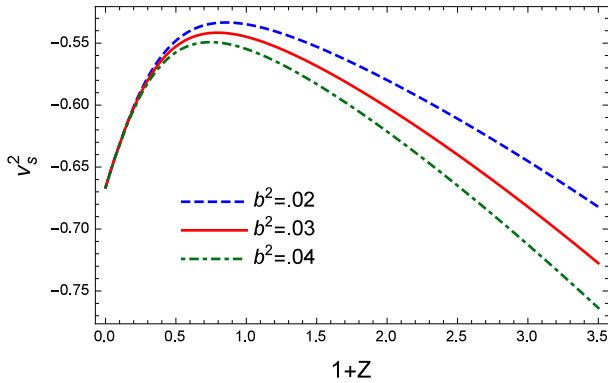


FIG. 11: The evolution of the squared of sound speed  $v_s^2$  versus redshift parameter  $z$  for interacting NTADE in HL cosmology. Here, we have taken  $\Omega_D(z=0) = 0.73$ ,  $H(z=0) = 67$ ,  $\Omega_k(z=0) = 0.01$ ,  $B = 2.4$ ,  $\lambda = 1.6$  and  $\delta = .2$

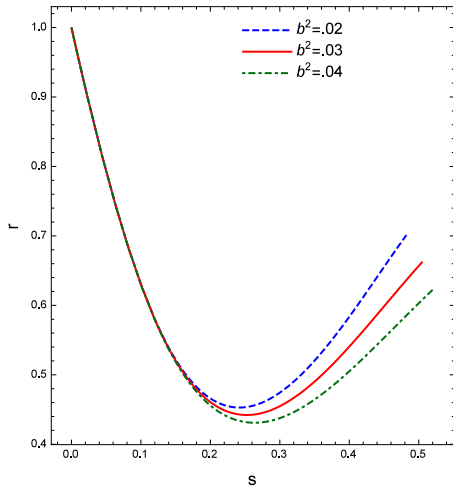


FIG. 12: The evolution of the statefinder parameter  $r$  versus  $s$  for interacting NTADE in HL cosmology. Here, we have taken  $\Omega_D(z=0) = 0.73$ ,  $H(z=0) = 67$ ,  $\Omega_k(z=0) = 0.01$ ,  $B = 2.4$ ,  $\lambda = 1.6$  and  $\delta = .2$

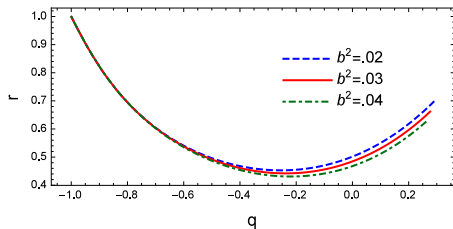


FIG. 13: The evolution of the statefinder parameter  $r$  versus the deceleration parameter  $q$  for interacting NTADE in HL cosmology. Here, we have taken  $\Omega_D(z=0) = 0.73$ ,  $H(z=0) = 67$ ,  $\Omega_k(z=0) = 0.01$ ,  $B = 2.4$ ,  $\lambda = 1.6$  and  $\delta = .2$

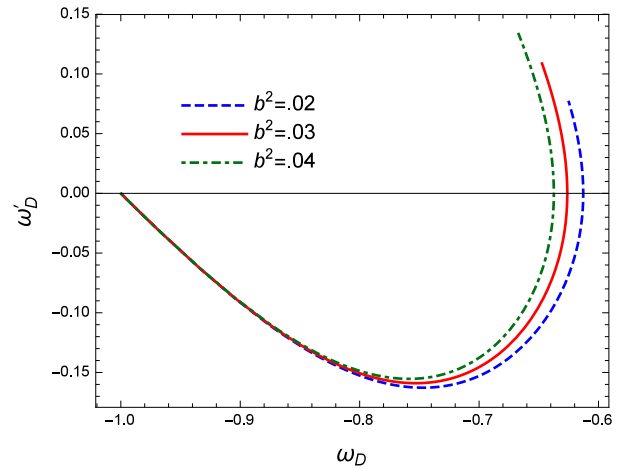


FIG. 14: The  $\omega_D - \omega'_D$  diagram for interacting NTADE in HL cosmology. Here, we have taken  $\Omega_D(z=0) = 0.73$ ,  $H(z=0) = 67$ ,  $\Omega_k(z=0) = 0.01$ ,  $B = 2.4$ ,  $\lambda = 1.6$  and  $\delta = .2$

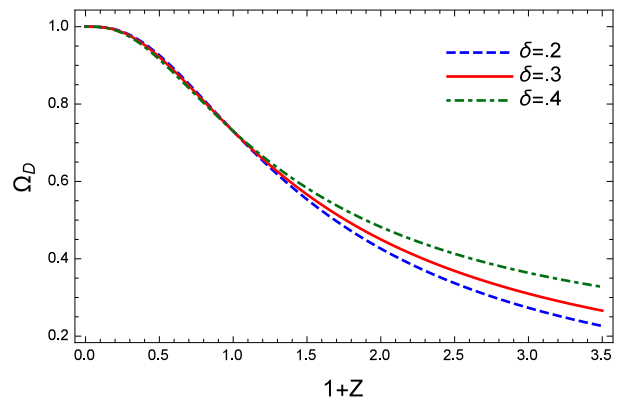


FIG. 15: The evolution of  $\Omega_D$  versus redshift parameter  $z$  for interacting NTADE in HL cosmology. Here, we have taken  $\Omega_D(z=0) = 0.73$ ,  $H(z=0) = 67$ ,  $\Omega_k(z=0) = 0.01$ ,  $B = 2.4$ ,  $\lambda = 1.6$  and  $b^2 = .02$

the future for different values of  $b^2$  as well as from Fig. 13, we see that the evolutionary trajectories started from matter dominated universe in the past and approach the point  $(r = 1, q = -1)$  in the future. The  $\omega_D - \omega'_D$  plane for TNADE model in HL cosmology, by considering different values of  $b^2$  has plotted in Fig. 14. We see that this model represents the freezing region. In Figs. 15-21, we show cosmological parameters for different values of  $\delta$  for interacting case. From Figs. 15-17, we see that  $\Omega_D$  trends to 1 at late time,  $\omega_D$  cannot cross phantom line and  $q$  shows a transition from the deceleration phase to the acceleration one. In Fig. 18, we have plotted  $v_s^2$  for different values of  $\delta$ . We observe that the model is unstable. We have plotted Figs. 19-21 for statefinder parameters and  $\omega - \omega'$  plane by considering different values of  $\delta$ . From Fig. 19, we observe that for  $(r - s)$  plane of NTADE, the statefinder parameters  $r$  and  $s$  end at

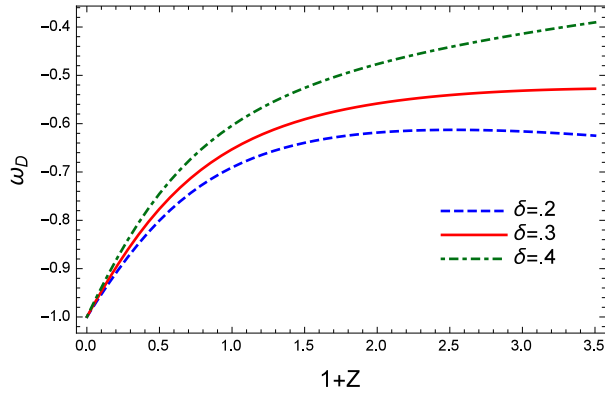


FIG. 16: The evolution of  $\omega_D$  versus redshift parameter  $z$  for interacting NTADE in HL cosmology. Here, we have taken  $\Omega_D(z=0) = 0.73$ ,  $H(z=0) = 67$ ,  $\Omega_k(z=0) = 0.01$ ,  $B = 2.4$ ,  $\lambda = 1.6$  and  $b^2 = .02$

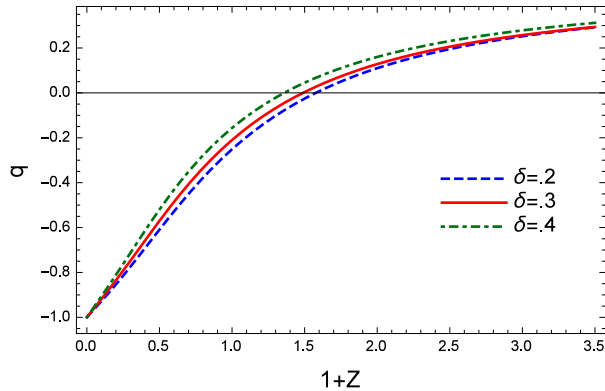


FIG. 17: The evolution of the deceleration parameter  $q$  versus redshift parameter  $z$  for interacting NTADE in HL cosmology. Here, we have taken  $\Omega_D(z=0) = 0.73$ ,  $H(z=0) = 67$ ,  $\Omega_k(z=0) = 0.01$ ,  $B = 2.4$ ,  $\lambda = 1.6$  and  $b^2 = .02$

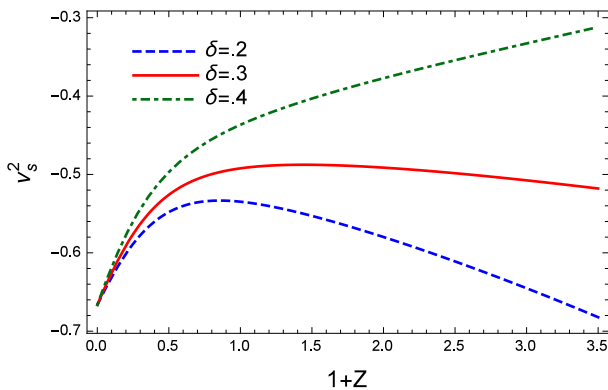


FIG. 18: The evolution of the squared of sound speed  $v_s^2$  versus redshift parameter  $z$  for interacting NTADE in HL cosmology. Here, we have taken  $\Omega_D(z=0) = 0.73$ ,  $H(z=0) = 67$ ,  $\Omega_k(z=0) = 0.01$ ,  $B = 2.4$ ,  $\lambda = 1.6$  and  $b^2 = .02$

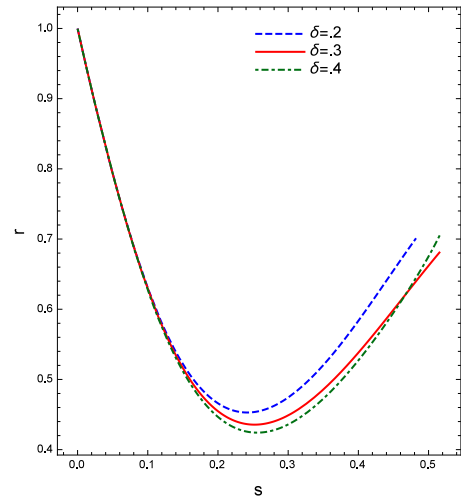


FIG. 19: The evolution of the statefinder parameter  $r$  versus  $s$  for interacting NTADE in HL cosmology. Here, we have taken  $\Omega_D(z=0) = 0.73$ ,  $H(z=0) = 67$ ,  $\Omega_k(z=0) = 0.01$ ,  $B = 2.4$ ,  $\lambda = 1.6$  and  $b^2 = .02$

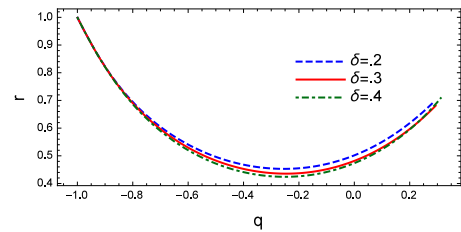


FIG. 20: The evolution of the statefinder parameter  $r$  versus the deceleration parameter  $q$  for interacting NTADE in HL cosmology. Here, we have taken  $\Omega_D(z=0) = 0.73$ ,  $H(z=0) = 67$ ,  $\Omega_k(z=0) = 0.01$ ,  $B = 2.4$ ,  $\lambda = 1.6$  and  $b^2 = .02$

$\Lambda$ CDM ( $r = 1, s = 0$ ) in the future by considering interaction term as well as in  $(r, q)$  evolutionary plane, we see that the evolutionary trajectories have started from matter dominated universe in the past and end their evolution in  $\Lambda$ CDM ( $r = 1, q = -1$ ). In Fig. 21, the  $\omega - \omega'$  plane shows the freezing region which correspond to accelerated expansion of the Universe.

#### IV. CLOSING REMARKS

In this paper, we have investigated the NTADE scenario in the framework of Horava-Lifshitz cosmology. Since ADE density corresponds to a dynamical cosmological constant, we used from a dynamical framework, instead of general relativity. Thus, we investigated the NTADE in the framework of Horava-Lifshitz cosmology. Since experimental data have implied that our universe is not a perfectly flat universe, we imposed an arbitrary curvature for the background geometry, and we allowed for



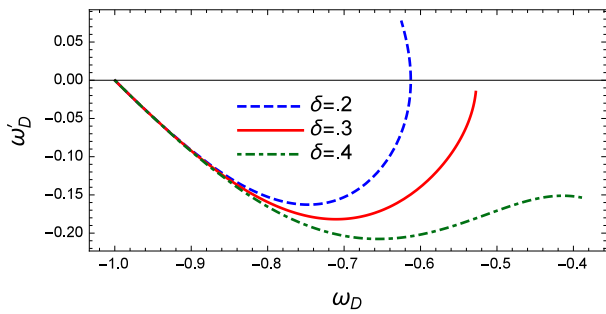


FIG. 21: The  $\omega_D - \omega'_D$  diagram for interacting NTADE in HL cosmology. Here, we have taken  $\Omega_D(z=0) = 0.73$ ,  $H(z=0) = 67$ ,  $\Omega_k(z=0) = 0.01$ ,  $B = 2.4$ ,  $\lambda = 1.6$  and  $b^2 = .02$

an interacting between the matter and dark energy sectors. For both non-interacting and interacting cases, we extracted the differential equation that determines the evolution of the dark energy density parameter, which gives a suitable estimate for the state parameter of dark energy as well as the deceleration parameter to study an expansion of the universe. Also, we studied statefinder trajectories and  $\omega - \omega'$  plane. To study parametric behaviour, we found that phantom crossing can not occur for the state parameter for small values of coupling parameter  $b^2$  and  $\delta$ , and from the plot of the deceleration parameter, we have observed a transition from decelerating to accelerating phase of the universe. Also, model is not stable while the cosmological plane can meet the freezing region.

- 
- [1] A.G. Riess, A.V. Filippenko, P. Challis, A. Clocchiatti, A. Diercks, P.M. Garnavich, R.L. Gilliland, C.J. Hogan, S. Jha, R.P. Kirshner, *et al.*, *The Astronomical Journal* **116**(3), 1009 (1998).
- [2] S. Perlmutter, G. Aldering, G. Goldhaber, R. Knop, P. Nugent, P. Castro, S. Deustua, S. Fabbro, A. Goobar, D. Groom, *et al.*, *The Astrophysical Journal* **517**(2), 565 (1999).
- [3] V. Sahni, *Lecture Notes in Physics* **653**(2), 141 (2004).
- [4] S.M. Carroll, *Living Reviews in Relativity* **4**(1), 1 (2000).
- [5] R. G. Cai, *Phys. Lett. B* **657**, 228 (2007) [arXiv:0707.4049].
- [6] H. Wei and R. G. Cai, *Phys. Lett. B* **660**, 113 (2008) [arXiv:0708.0884].
- [7] J. P. Wu, D. Z. Ma and Y. Ling, *Phys. Lett. B* **663**, 152 (2008) [arXiv:0805.0546].
- [8] E.M. Lifshitz, *Zh. Eksp. Teor. Fiz.* **11**, 255 (1949).
- [9] P. Horava, *Phys. Rev. D* **79**, 084008 (2009) [arXiv:0901.3775];  
P. Horava, *Phys. Rev. Lett.* **102**, 161301 (2009) [arXiv:0902.3657].
- [10] J. Greenwald, J. Lenells, J.X. Lu, V.H. Satheeshkumar, A. Wang, *Phys. Rev. D* **84**, 084040 (2011).
- [11] B. Chen, S. Pi and J. Z. Tang, , [arXiv:0910.0338].
- [12] S. Nojiri and S.D. Odintsov, *Phys. Rev. D* **81**, 043001 (2010) [arXiv:0905.4213].
- [13] J. Kluson, *JHEP* **11**, 078 (2009) [arXiv:0907.3566].
- [14] A. Wang and Y. Wu, *JCAP* **07**, 012 (2009) [arXiv:0905.4117].
- [15] S. Mukohyama, K. Nakayama, F. Takahashi and S. Yokoyama, *Phys. Lett. B* **679**, 6 (2009) [arXiv:0905.0055].
- [16] M. I. Park, *JCAP* **01**, 001 (2010) [arXiv:0906.4275].
- [17] M. Fukushima, Y. Misonoh, S. Miyashita, S. Sato, *Phys. Rev. D* **99**, 064004 (2019).
- [18] A. Tawfik, E. Abou El Dahab, *Int. J. Theor. Phys.* **56**, 2122-2139 (2017).
- [19] Y. Heydarzade, M. Khodadi, F. Darabi, *Theor. Math. Phys* **190**, 130 (2017).
- [20] Nils A. Nilsson, *et al.*, *Physics of the Dark Universe* **23C**, 100253 (2019).
- [21] G. Cognola, *et al.*, *Class. Quant. Grav.* **33** 225014 (2016).
- [22] Tao Zhu, *et al.*, *Phys.Rev. D* **84** 101502 (2011).
- [23] Tao Zhu, *et al.*, *Phys.Rev. D* **85** 044053 (2012).
- [24] Tao Zhu, *et al.*, *JHEP* **1301** 138 (2013).
- [25] Tao Zhu, *et al.*, *Phys.Rev. D* **88** 063508 (2013).
- [26] Karami, K., Jamil, M., Roos, M., Ghaffari, S., Abdolmaleki, A. *Astrophys. Space Sci.* **340**, 175 (2012).
- [27] Jamil, M., Saridakis, E.N., Setare, M.R.J. *Cosmol. Astropart. Phys.* **11**, 32 (2010)
- [28] Jamil, M., Saridakis, E.N.J. *Cosmol. Astropart. Phys.* **7**, 28 (2010)
- [29] S. F. Bramberger, A. Coates, J. Magueijo, S. Mukohyama, R. Namba and Y. Watanabe, *Phys. Rev. D* **97**, no. 4, 043512 (2018).
- [30] J. Bellorin, A. Restuccia and F. Tello-Ortiz, *Phys. Rev. D* **98**, no. 10, 104018 (2018).
- [31] E. M. C. Abreu, A. C. R. Mendes, G. Oliveira-Neto, J. Ananias Neto, L. G. R. Rodrigues and M. Silva De Oliveira, arXiv:1805.11042 [gr-qc].
- [32] R. Maier and I. D. Soares, *Phys. Rev. D* **96**, no. 10, 103532 (2017).
- [33] Genly Leon, *et al.* arXiv:1902.09961v3 [gr-qc]
- [34] Tanwi Bandyopadhyay, *et al.* arXiv:1908.11720v1 [gr-qc].
- [35] J. W. Gibbs, (C. Scribners Sons, New York, 1902); Yale University Press.
- [36] C. Tsallis, *J. Stat. Phys.* **52**, 479 (1988).
- [37] C. Tsallis, L. J. L. Cirto, *Eur. Phys. J. C* **73**, 2487 (2013)
- [38] M. Abdollahi Zadeh, A. Sheykhi, H. Moradpour, and K. Bamba, *Eur. Phys. J. C*, **78**, 940 (2018).
- [39] Abdollahi Zadeh, M., Sheykhi, and A. Moradpour, *H. Gen. Relativ. Gravit.* **51**, 12 (2019).
- [40] S. Ghaffari *et al.*, *Eur. Phys. J. C* **78**, 706 (2018).
- [41] S. Ghaffari *et al.*, *Phys. Dark. Univ.* **23**, 100246 (2019).
- [42] S. Nojiri, S. D. Odintsov, and E. N. Saridakis, *Eur. Phys. J. C* **79**, 242 (2019).
- [43] E. N. Saridakis, K. Bamba, R. Myrzakulov, and F. K. Anagnostopoulos, *JCAP* **1812**, 012 (2018).
- [44] G. Varshney, U. K. Sharma, and A. Pradhan, *New Astronomy* **70**, 36 (2019).
- [45] M. Abdollahi Zadeh, A. Sheykhi, H. Moradpour, and

- K. Bamba, *Mod. Phys. Lett. A* **33**, 2050053 (2020). [arXiv:1901.05298v1]
- [46] V. C. Dubey, U. K. Sharma, and A. Beesham, [arXiv:1905.02449v1]; V. C. Dubey, S. Srivastava, U. K. Sharma, and A. Pradhan, *Pramana J. Phys.* **93**, 78 (2019); V. C. Dubey, A. K. Mishra, S. Srivastava, U. K. Sharma, *Int. J. Geom. Method. Mod. Phys.* DOI: 10.1142/S0219887820500115 (2019).
- [47] N. Zhang, Y. B. Wu, J. N. Chi, Z. Yu, and D. F. Xu, [arXiv:1905.04299v2]
- [48] U. K. Sharma, V. C. Dubey, and A. Pradhan, [arXiv:1906.08051v1]
- [49] C. Q. Geng, Y. T. Hsu, J. R. Lu, and L. Yin, [arXiv:1911.06046v1]
- [50] R. D'Agostino, *Phys. Rev. D* **99**, 103524 (2019)
- [51] M. Sharif, S. Saba, *Symmetry*, **11**(1), 92 (2019)
- [52] Q. Huang et al, *Class. Quantum Grav.* **36** 175001 (2019)
- [53] W. J. C. da Silva, and R. Silva, *JCAP* **05**, 036 (2019)
- [54] A. V. Astashenok, and A. S. Tepliakov, [arXiv:1911.01422v1]
- [55] M. Korunur, *Modern Physics Letters A* Vol. **34**, No. **37** (2019) 1950310 (12 pages). DOI: 10.1142/S0217732319503103
- [56] Y. Adityaa, S. Mandalb, P. K. Sahoo, and D. R. K. Reddy, [arXiv:1910.12456v1]
- [57] A. A. Aly, *Advances in Astronomy*, Article ID 8138067 (2019)
- [58] K. Ourabah, E. M. Barboza, E. M. C. Abreu, and J. A. Neto, *Phys. Rev. D* **100**, 103516 (2019).
- [59] S. R. M. Younas, A. Jawad, S. Qummer, H. Moradpour, *AHEP* 1287932, (2019).
- [60] H. Moradpour, *Int. J. Theor. Phys.* **55**, 4176 (2016).
- [61] G. Calcagni, *JHEP* **09**,112 (2009) [arXiv:0904.0829] ; E. Kiritsis and G. Kofinas, *Nucl. Phys. B* **821**, 467 (2009) [arXiv:0904.1334].
- [62] P. Horava, *Phys. Rev. D* **79**, 084008 (2009) . [arXiv:0901.3775].
- [63] S. M. Carroll and E.A. Lim, *Phys. Rev. D* **70**, 123525 (2004).
- [64] M. Abdollahi Zadeh, A. Sheykhi and H. Moradpour, *Mod. Phys. Lett. A* **34**, no. 11, 1950086 (2019).
- [65] R. G. Cai, *Phys. Lett. B* **657**, 228 (2007).
- [66] V. Sahni, T. D. Saini, A. A. Starobinsky and U. Alam, *JETP Lett.* **77**, 201 (2003).
- [67] R. Caldwell and E. V. Linder, *Phys. Rev. Lett.* **95**, 141301 (2005).
- [68] E. Komatsu *et al.*, *Astrophys. J. Suppl.* **180**, 330 (2009); J. P. Uzan, U. Kirchner, and George F. R. Ellis, *Mon. Not. R. Astron. Soc.* **344**, L65L68 (2003).
- [69] P. J. Steinhardt, *Cosmological challenges for the 21st century, in Critical problems in physics*, V. L. Fitch and D. R. Marlow eds., Princeton University Press, Princeton U.S.A. (1997).
- [70] O. Bertolami, F. Gil Pedro, and M. Le Delliou. *Phys. Lett. B*, **654**, 165 (2007); M. Baldi. *Mon. Not. R. Astron. Soc.* **414**, 116 (2011).
- [71] M. Jamil and M. A. Rashid. *Eur. Phys. J. C*, **56**, 429 (2008).
- [72] J. H. He and B. Wang, *JCAP* **06**, 010 (2008).
- [73] J. H. He, B. Wang, and Y. P. Jing, *JCAP* **07**, 030 (2009).
- [74] X. D. Xu, B. Wang, P. Zhang, and F. A. Barandela, *JCAP*, **12**, 001 (2013).
- [75] B. Wang, E. Abdalla, F. Atrio-Barandela and D. Pavon, *Rep. Prog. Phys.* **79**, 096901 (2016).